View metadata, citation and similar papers at core.ac.uk

brought to you by CORE

provided by Harvard University - DASH

DIGITAL ACCESS TO SCHOLARSHIP AT HARVARD
DASH.HARVARD.EDU

HARVARD LIBRARY
Office for Scholarly Communication

Circulating Micro-RNAs as Biomarkers for Thoracic Radiation Therapy in Lung Cancer

The Harvard community has made this article openly available. Please share how this access benefits you. Your story matters

Citation	Dinh, Tru-Khang T. 2016. Circulating Micro-RNAs as Biomarkers for Thoracic Radiation Therapy in Lung Cancer. Doctoral dissertation, Harvard Medical School.
Citable link	http://nrs.harvard.edu/urn-3:HUL.InstRepos:27007756
Terms of Use	This article was downloaded from Harvard University's DASH repository, and is made available under the terms and conditions applicable to Other Posted Material, as set forth at http://nrs.harvard.edu/urn-3:HUL.InstRepos:dash.current.terms-of-use#LAA

Acknowledgements

I am indebted to my mentors, Dr. David Kozono and Dr. Alan D'Andrea, for their support and guidance. This work would also not be possible without the encouragement, patience, and love of my wife, Kathryn. Finally, I would not have the privilege of being where I am today without the sacrifices made by my parents, who taught me how one can lose it all and still live a life of dignity, meaning, and hope.

Abstract

Risk of normal tissues toxicity limits the amount of thoracic radiation therapy that can be routinely prescribed for the treatment of non-small cell lung cancer (NSCLC). An early biomarker of response to thoracic radiation may provide a way to predict eventual toxicities during the multi-week treatment regimen. This enables dose adjustment before the symptomatic onset of late effects, such as radiation pneumonitis and esophagitis. Micro-RNAs (miRNAs) are small, non-coding RNAs that regulate gene expression by decreasing the translation of messenger RNAs. miRNAs constitute a major fraction of small RNAs reproducibly found in circulation, in part due to their protective encapsulation within exosomes. They are therefore attractive candidates as serological biomarkers. In this study, we performed miRNA profiling of the blood of 5 NSCLC patients at 5 dose-points during thoracic RT and found 10 miRNAs that correlated well with total radiation dose as well as other common dosimetric parameters. We then assessed these 10 miRNAs in samples from a separate cohort of 21 NSCLC patients receiving RT and identified miR-29a-3p and miR-150-5p as potential, reproducible biomarkers that decreased in circulation with increasing radiation dose. We also conducted *in-vitro* experiments to measure the expression levels of these miRNAs intracellularly and within exosomes in three NSCLC cell lines and two lung bronchoepithelial and fibroblast lines. The exosomal expression of miR-29a-3p and miR-150-5p decreased with radiation. However, this was concomitant with an increase in intracellular levels, suggesting that exosomal export of these miRNAs may be downregulated in NSCLC and stromal cells as a response to radiation. One may therefore hypothesize that outlier trends in levels of circulating miR-29a-3p and miR-150-5p may predict unexpected responses to radiation therapy, such as toxicity.

Table of Contents

Glossary

1. Gy: Gray = one Joule per Kilogram
2. NSCLC: non-small cell lung cancer
3. miRNA, MiR: micro-RNA
4. RTOG: Radiation Therapy Oncology Group
5. RT: radiation therapy
6. RP: radiation pneumonitis
7. QUANTEC: Quantitative Analyses of Normal Tissue Effects in the Clinic
8. MLD: mean lung dose
9. V20: percent of total lung volume exposed to at least 20 Gy of radiation
10. V5: percent of total lung volume exposed to at least 5 Gy of radiation
11. TGF-β1: transforming growth factor beta 1
12. IL-1/6: interleukin 1/6
13. MVB: multi-vesicular bodies
14. cDNA: complementary deoxyribonucleic acid
15. EBV: Epstein Barr virus
16. FBS: fetal bovine serum
17. RPMI: Roswell Park Memorial Institute
18. TCGA: Tumor Cancer Genome Atlas
19. GEO: Gene Expression Omnibus
20. GSEA: Gene Set Enrichment Analysis

Introduction

In 2015, an estimated 221,200 Americans will be diagnosed with lung cancer and 158,040 will die of the disease (1). Roughly 85% of lung cancers are non-small cell lung carcinomas (NSCLC), which are most often locally advanced (Stage III) or metastatic (Stage IV) at the time of diagnosis (2). Platinum-based chemotherapy with concurrent radiotherapy (RT) comprise first-line treatment for locally advanced NSCLC and has been shown to increase survival (3). However, despite optimal chemoradiotherapy, rates of loco-regional recurrence remain high and patients often suffer treatment failure within the irradiated area in approximately 40% of cases (4). Indeed, the 5-year mortality rate for Stage III NSCLC is a dismal 15-25% (5, 6). Attempting to improve survival rates, the Radiation Therapy Oncology Group undertook a trial (RTOG 0617) which randomized patients to receive 60 Gy, the standard dose, or a higher 74 Gy dose of radiation to observe whether dose escalation improves outcomes (7). Unfortunately, there was no survival benefit to receiving the higher dose of radiation and there was even a higher number of absolute mortality in this arm. Furthermore, despite sometimes compromising tumor coverage to meet normal tissue constraints, the rates of esophagitis was higher in the dose-escalation arm compared to the standard dose arm.

A major reason why NSCLC recurs loco-regionally as frequently as it does is our inability to predict which patients may require dose escalation for better local control, or those who can tolerate higher RT doses to organs-at-risk. Despite complex variations in anatomic and biological characteristics between patients and their tumors, RT regimens have remained relatively uniform. Currently, the standard recommended radiation dose is 60 Gy given in 2.0 Gy daily fractions, based on the results of RTOG 0617 (7). In practice however, prescriptions range between 60-70 Gy in 1.8 to 2.0 Gy daily fractions, depending on provider preferences as well as dosimetric constraints related to extent of tumor infiltration of or proximity to radiosensitive structures such as the lungs, spinal cord, esophagus and heart (8). Particularly in the treatment of NSCLC, collateral damage to normal lung tissue is a major concern that often limits the achievable dose, likely to the detriment of local disease control. It has been reported that between 10 and 20 percent of patients suffer moderate or severe radiation-induced pneumonitis (RP) following standard

treatments (9). RP is an inflammatory response of the lungs resulting in symptoms of variable severity ranging from subclinical changes only detectable on imaging to chronic cough, dyspnea, low-grade fever, or even pulmonary failure requiring hospitalization. Moreover, this figure is likely to be underestimated since the clinical manifestations of RP are highly non-specific and common symptoms. In severe cases, the RP-attributed mortality rate can be as high as 50% (10).

The Quantitative Analyses of Normal Tissue Effects in the Clinic (QUANTEC) meta-analysis collated previous attempts to balance the need for adequate tumor control with normal lung toxicity by identifying dosimetric parameters, such as mean lung dose (MLD) and Vx (percent volume of both lungs receiving at least x dose of radiation; most often 20 Gy or V20), which could predict RP and other endpoints of normal-tissue toxicity such as esophagitis and coronary fibrosis (8). The study confirmed that higher indices of radiation exposure generally correlated with increasing probability of symptomatic pneumonitis. Unfortunately, the study failed to identify any reliable threshold above which RP was likely. Indeed, rates of symptomatic RP varied widely between different retrospective studies at any particular MLD or Vx. This limitation in using dosimetric parameters to minimize toxicity has led to significant differences in practice patterns between radiation therapy groups. It is likely that rates of radiation-induced toxicity will also vary, based upon institutional experience and provider preference. To improve patient outcomes, a more reliable predictor of toxicity (or conversely, of tumor response) is required.

More recent efforts have focused on biochemical markers that potentially correspond to normal-tissue toxicities (11). Naturally, inflammatory cytokines that could be measured in the circulation were attractive candidates. Levels of circulating TGF-β1 were explored as a potential biomarker of RP. Li and colleagues measured pre-RT levels of both soluble TGF-β1 and ligand-receptor complexes between TGF-β1 and one of its receptors, CD105, in 91 patients treated for breast cancer (12). They found that patients with higher pre-radiotherapy plasma levels of TGF-β1 and lower levels of ligand-receptor complexes were more likely to develop fibrosis of breast tissue. The authors suggested a cutoff value of 96 pg/ml for TGF-β1, which predicted breast fibrosis with a sensitivity of 76% and specificity of 74%. In the lung, Anscher and colleagues measured TGF-β1 before, during, and after RT in 73 patients with NSCLC (13). They were unable to ascertain a

reliable TGF-β1 threshold that predicted pneumonitis, although patients whose post-RT TGF-β1 had renormalized to pre-treatment levels were less likely to suffer from RP with a positive predictive value of 90%. A subsequent, prospective trial from two institutions examined the ratio of TGF-β1 during RT compared to pre-RT as a predictive biomarker of radiation-induced lung toxicity (14). In 165 patients, a TGF-β1 ratio of greater than 1 performed significantly better than MLD in predicting patients who go on to suffer from RP. Unfortunately, the specificity of this approach was severely limited, as 53.8% of patients with TGF-β1 ratio greater than 1 did not suffer from RP.

Based on these encouraging results suggesting that TGF-β1 as a biomarker may be superior to doximetric parameters in predicting RP, Anscher and colleagues attempted a prospective dose-escalation trial for lung cancer patients whose TGF-β1 levels had returned to baseline levels at the end of standard-dose RT (15). Patients whose serum TGF-β1 returned to baseline after a standard course of RT of 73.6 Gy received additional treatments up to 86.4 Gy. This trial showed that patients with elevated post-RT TGF-β1 still developed more severe lung toxicity, despite being spared additional radiation. Unfortunately, large fractions of patients in the TGF-β1 -guided dose-escalation arms also still experienced RP during follow-up despite having renormalized TGF-β1 levels. Later studies have shown that TGF-β1 levels actually correlated with tumor volume (likely because tumors produced TGF-β1), and therefore the volume of lung irradiated, which rather than being predictive for RP, was already demonstrated by QUANTEC to be an unreliable marker (16, 17).

Other investigators have focused on the cytokines, IL-1 and IL-6, as potential biomarkers to predict normal-tissue toxicity after RT (11). Chen et al found that circulating levels of IL-6 were higher before, during, and after RT in a small group of patients who developed mild RP (18). However, the sensitivity and specificity of IL-6 to retrospectively predict RP was only 78% and 40%, respectively (19). Furthermore, comparing post-RT to pre-RT IL-6 levels did not perform any better as a predictor than simply measuring baseline IL-6 levels. Finally, Stenmark et al. attempted to combine dose-volume histogram parameters with inflammatory cytokines in order to improve the prediction of RP (20). They were able to slightly improve RP sensitivity (80%), but still reported low specificity (60%).

In recent years, micro-RNAs (miRNAs) have garnered interest as potential biomarkers for a range of biological and physiological states(21). miRNAs are small (22-24 nucleotide), non-coding RNAs that serve to modulate gene expression by decreasing the expression levels of as many as 60% of all coding sequences in the human genome via many components of the small-interfering RNA (siRNA) effectors pathway (22-24). Mature miRNA can bind to Argonaute as part of the RNA-induced silencing complex (RISC) in order to identify and cleave complementary mRNA. Alternatively, miRNA can bind to complementary segments of nucleotides within its target mRNA, most often in the 3' untranslated regions (UTR), to decrease the efficiency of protein translation. The sequence complementation between miRNAs and the mRNAs they target are remarkably conserved between species. Circulating miRNAs are attractive as potential biomarkers of tumor radiation response and normal-tissue toxicity. They constitute the major fraction of small nucleic acids found in circulation, and despite the high concentration of RNA-degrading enzymes, circulating miRNA expression levels have been measured to be stable, reproducible, and consistent (21). miRNA expression has been shown to significantly and specifically change in murine serum following whole body radiation (25, 26). Further, miRNA expression in peripheral blood cells has been used to accurately distinguish pre- and post-radiation states in human patients (27). While the exact mechanisms underlying these changes are currently under investigation, miRNAs have been shown to be involved in regulating the DNA damage response, making it especially relevant in the context of RT for NSCLC (28).

Despite being widely reported as potential biomarkers for a range of physiologic processes, the origins of circulating miRNAs have not been well studied. It has been recently shown that the majority of circulating miRNAs in serum are found within exosomes, which protect miRNAs from degradation (29, 30). Exosomes are small (50-80nm) membrane vesicles of endocytic origin that are formed by the inward budding of endosomes into multi-vesicular bodies (MVB) (31). Mature MVBs subsequently fuse with the plasma membrane to release exosomes from the cell in an orchestrated manner that is distinct from exocytosis. Exosomes containing miRNAs have been shown to travel in an antigen-specified, unidirectional manner from T cells to antigen presenting cells during the formation of an immune synapse (32). Interestingly, these exosomes communicate a

different set of miRNAs than those found in their parent T cells and serve to modulate gene expression in the target cells. Further highlighting the importance of miRNA-containing exosomes as mediators of intercellular communication are co-culture experiments of EBV-infected and uninfected cells (33). These experiments showed that non-infected cells internalize exosomes secreted by EBV-infected B cells and subsequently down-regulate the expression of immunomodulatory genes confirmed to be critical in EBV-associated lymphoma transformation, most notably *CXCL11/ITAC*.

The complementary mechanisms by which miRNAs regulate mRNA expression make it possible to computationally predict gene targets of any particular miRNA. The most validated algorithm for performing target prediction is Targetscan, which has been shown to have performance rivaling experimental methods (34, 35). Targetscan identifies mRNA sequences that are likely to be targets of a specific miRNA by generating a context score which takes into account 14 validated features of miRNA-target mRNA binding and recognition. This tool makes it possible to quickly investigate changes in genetic expression due to any observed differences in miRNA expression. With the proliferation of gene expression profiles that are publically available, genome target prediction makes it possible to infer the genotypic results of any particular miRNA signature. miRNA signals can then be indirectly correlated to phenotypic classes, such as treatment exposure in radiation therapy. While investigators should be cautious when performing combined analyses of multiple expression datasets, this approach could be useful in generating hypotheses for further studies.

In this study, we hypothesized that miRNA expression in the peripheral circulation may serve as biomarkers for radiation response during thoracic RT in NSCLC patients. We also investigated the potential cellular source of miRNAs in circulation by measuring miRNA expression in exosomes from cells and conditioned media. Finally, gene set enrichment analysis of predicted targets of potential miRNA biomarkers were performed on previously published gene expression microarrays. miRNA biomarkers that are identified as radiation-responsive may correspond to tumor response or damage to irradiated organs-at-risk, allowing prediction of acute and delayed injury to these organs. Such a tool has the potential advance the goal of rationally tailoring RT for NSCLC patients who would tolerate and/or need dose-escalation for local disease control.

Materials and Methods

miRNA profiling and validation:

Five plasma samples from each of five patients with Stage IIIA NSCLC treated with radical chemoradiotherapy (profiling cohort) were collected before—and at roughly 2 week intervals during—RT (Table 1). 10 mL of blood were collected in K-EDTA coated Vacutainer tubes (Fischersci). Whole blood was transferred to 15mL conical tubes and immediately spun at 2000xg for 15min at 4C. The resulting platelet-depleted plasma was aspirated and aliquoted into 500ul volumes and stored in 1.5mL cryo vials at -80 deg C. Samples were comprehensively profiled for known human miRNAs (~1900) using Exiqon miRCURY LNA Universal RT microRNA PCR Human Panel I+II arrays. Candidate miRNAs whose levels significantly correlated with RT dose, lung V5, lung V20, mean lung dose, and mean esophagus dose were identified. miRNA candidates identified in the screen were validated using samples from the original screening cohort and an additional 21 NSCLC patients (validation cohort), collected before—and at 20Gy intervals during—RT. Patients in the validation cohort had similar disease characteristics and treatment regimens (Table 2). All patients in the profiling cohort underwent concurrent chemoradiation while 10 of 21 patients in the validation cohort received radiation in the adjuvant setting. One sample each from the 0 Gy and 40 Gy groups as well as two from the 20 Gy group had undetectable levels of miRNAs, likely due to degradation during processing or transport.

For both screening and validation cohort plasma samples, total RNA was isolated from 200 uL volumes of plasma samples using Exiqon miRCURY Biofluids Total RNA Isolation kits (Exiqon, Copenhagen, Denmark). cDNA synthesis was performed for all samples using Universal cDNA first-strand synthesis kits (Exiqon) by adding 4μL of total RNA. Quantitative real time-PCR was performed using the Exiqon SYBR Green system in a 96-well format. All LNA primers were ordered from Exiqon and added at 250nM final concentration in the reaction mixture.

Measurement of significant miRNAs in cells and conditioned media:

Human NSCLC cell lines NCI-H460 (large-cell lung carcinoma), A549 (type II alveolar cell carcinoma), and NCI-H1299 (lung adenocarcinoma) as well as diploid,

embryonic-derived MRC5 (lung epithelial fibroblasts) and IMR90 (lung epithelial fibroblasts) cells were grown in 10 cm tissue culture plates (36-40). NSCLC cells were cultured in Roswell Park Memorial Institute (RPMI) 1640 (Life Technologies) media supplemented with 10% fetal bovine serum (FBS, Sigma). MRC5 and IMR90 cells were cultured in Eagle's Modified Essential Media (ATCC, Manassas, USA) supplemented with 10% FBS. To minimize changes in miRNA expression due to serum starvation, cells were maintained throughout in complete media. Because some miRNAs have been detected in FBS, the same batch of FBS was used for all in-vitro experiments. Additionally, media with FBS were profiled for miRNAs of interest for background normalization (Figure 1).

For measurement of intracellular miRNA expression, cells were transferred to 6-well tissue-culture plates (Thermofisher, Waltham, USA) at a density of 10^5 cells per well and allowed to reach log-phase growth in 48 h. Samples (n=6 per group) were then irradiated using a Gammacell 40 Exactor (Best Theratronics) with 2 Gy per day for 1,2, or 3 days (2 Gy, 4 Gy, or 6 Gy total dose). Each day, cells were trypsinized and harvested 2 hours after irradiation.

For measurement of extracellular miRNA expression in conditioned media, cells were transferred to 15cm tissue-culture plates (Falcon) at a density of 10^6 cells per plate and allowed to reach log-phase growth in 48 h. Samples (n=3 per group) were then irradiated at 2Gy per day for 1 and 3 days (2Gy or 6Gy total dose). Fresh media was added one hour prior to radiation on day 1 and media was not changed subsequently. After days 1 and 3, 10 mL conditioned media was collected from each plate 2 h after irradiation. Cellular debris was removed by centrifugation at 3200 x g for 10 minutes before the supernatant was stored at -70°C for downstream miRNA quantification. Exosomes were isolated and purified using a solvent-exchange exosome isolation kit (Exiqon) before total RNA was isolated with Plant and Cells Total RNA Isolation kits. Isolation of exosomes was confirmed by Western Blotting for Tsg101, a protein involved in multi-vesicular biogenesis (29, 41).

After sample collection, total RNA was immediately isolated from cell pellets using Exiqon miRCURY Plant and Cells Total RNA Isolation kits. cDNA synthesis was performed using Exiqon Universal cDNA first-strand synthesis kits by adding 100 ng total RNA for intracellular samples and 6.5 µL total RNA for exosome samples. Quantitative RT-PCR was

performed using Exiqon SYBR Green master mix. All LNA primers except miR-150-5p were ordered from Exiqon and added at 250nM final concentration. Q-PCR was performed using an AB-7500 thermocycler. For miR-150-5p, the Qiagen miSCRIPT SYBR Green primer assay was used, RT was performed using the miSCRIPT RT Kit (Qiagen) and Q-PCR was performed using the miSCRIPT SYBR Green Kit (Qiagen). Relative miRNA expression of biological replicates was calculated using the $\Delta\Delta C_t$ method (42).

Cell viability was determined using the Trypan blue dye exclusion method, using a standard protocol (43). Cell proliferation was assessed by manually counting adherent cells, averaged over 5 random high-powered field (40x).

Normalization and Technical Controls

Due to the lack of endogenous controls that normalize the amount of a miRNA of interest to the total amount of miRNAs (such as actin or tubulin for mRNA), the selection of appropriate normalizers is critical to quantifying miRNA expression (44). When profiling data comprising many miRNAs are available, the average expression of all miRNAs in each sample is often used as the normalizer. Alternatively, a basket of miRNAs whose expression are most consistent between samples can be used to normalize (45). In the latter case, a different set of normalizers must be identified in each experiment. Normfinder is a statistical software that assigns a relative measure of "stability" based upon the variance of a miRNA's expression between samples in an experiment (46).

In the profiling cohort, the global average expression of all detectable miRNAs were used to normalize. In the validation cohort, miR-let-7d, miR-324, miR-16-2-3p, and miR-126 were used as normalizers based upon their universal expression in all samples and high Normfinder stability. For normalization of intracellular miRNA expression, the snRNA sequence U6 and miR-103a have been established as normalizers for quantification of intracellular miRNAs and were measured in addition to the two most stably expressed miRNAs from the initial screen, miR-let-7d and miR-16-2-3p, as putative normalizers (44). These four miRNAs were measured in each intracellular experiments and the two most stably expressed miRNAs—as assessed by Normfinder in each experiment—were used for normalization. For normalization of exosomal miRNA expression, miR-let-7a-5p has been shown to perform well as a normalizer for miRNA quantification of exosomes derived from

cell culture and was measured to potentially supplement miR-let-7d and miR-16-2-3p (47). These three miRNAs were measured in each intracellular experiments and the two most stably expressed miRNAs—as assessed by Normfinder in each experiment—were used for normalization.

Hemolysis is another issue which may confound the quantitative analysis of cell-free, circulating miRNA (48). As previously described by Blondal and colleagues, the difference in miR-451 and miR-23a expression in plasma samples was used to assess the degree of hemolysis. In this study, a cutoff value of greater than 8 was used to exclude samples that are likely to be hemolyzed.

Synthetic RNA and DNA were added to every sample to assure that RNA isolation, cDNA synthesis, and Q-PCR reactions were indeed consistent. For the profiling cohort samples, UniSp2, UniSp4, and UniSp5 were used as RNA isolation spike-in controls. UniSp6 was used as cDNA synthesis spike-in controls. Additionally, the DNA spike-in UniSp3 was added. In the validation cohort samples, UniSp3 and UniSp6 were used as spike-in controls. In all samples, spike-in controls were assayed at steady levels.

Computational Target Identification and Gene Set Enrichment Analysis

TargetScan (v7.0) was used to identify genes that are likely targeted by potential miRNA biomarkers. The gene targets for each miRNA with a context score of less than -0.8 were included in a custom miRNA gene list (less negative scores correspond to higher likelihood of miRNA-mRNA interaction). Expression profiles available on the Genome Expression Omnibus (GEO) (http://www.ncbi.nlm.nih.gov/gds, last accessed January 29, 2016) were abstracted using the search query: “lung cancer” OR “non-small cell lung cancer” AND “radiation”. Microarray data were selected from experiments where NSCLC tumor cells were exposed to clinically-relevant gamma radiation. Data were pre-processed to exclude unavailable or background values. Gene set enrichment analysis (GSEA v.2.2.1) was then performed on the selected gene expression data and custom miRNA target gene set using a published software package (49, 50). Samples were divided into two phenotypes: control (non-irradiated) and 24 h after irradiation. 1000 permutations were simulated on the phenotype and the weighted enrichment statistic was used. The cutoff for

significance of gene set enrichment was a false discovery rate (FDR) of 25%, which incorporates adjustment for multiple comparisons testing.

Statistical Methods:

In the profiling experiment, miRNA expression data were normalized toward the average expression of miRNAs detectable in all profiling samples. Using those miRNAs for normalization, we calculated dCp values by mean-centering all Cp values, using the formula,

$$dCp = \frac{\sum_{i=1}^{n} Cp(i^{th}\ miRNA)}{n} - \ Cp(miRNA\ of\ interest)$$

Thus, higher scores represent higher expression levels. Fold changes of relative expression were calculated using the $\Delta\Delta C_t$ method (42).

In the profiling experiment using the screening cohort, we used analysis of variance (ANOVA) to identify miRNAs whose expression differed significantly depending on the dose of radiation. The Benjamini-Hochberg step-up method was used to adjust significance values for multiple comparisons testing (51). miRNAs that showed significance in ANOVA, were selected for the validation experiments. For the validation experiment, we identified four miRNAs that were stably expressed in all screening cohort samples and did not correlate significantly with radiation dose.

Analysis in the validation cohort was performed using 63 samples from 21 patients treated for locally-advanced NSCLC to verify whether the observed differences replicate in that cohort as well. Given the larger number of patients and repeated measures at pre-specified time points we were able to use repeated measures ANOVA to estimate the association between radiation dose and miRNA levels while taking into account individual-specific patterns. We performed pairwise comparisons between the baseline, 20Gy and 40Gy time points using the Newman-Keuls test. We subsequently evaluated correlations between miRNA and dosimetry parameters to determine the pattern of changes of miRNAs differentially expressed in the profiling experiment. Pearson's correlation was used to evaluate the direction and strength of such correlations.

For in-vitro data, we used Student's t-test to compare miRNA expression levels between groups. In all cases, we assumed p levels < 0.05 to be statistically significant.

Results

Profiling of patient blood samples identifies two circulating miRNAs that inversely correlate with RT dose

Of 752 miRNAs profiled in at least one sample in the screening cohort, 124 were universally detected in all 25 samples. 4 samples were excluded at pre-processing due to hemolysis. Ten miRNAs differed significantly depending on the received RT dose (Figure 2). Of these 10 miRNAs, miR-150-5p (p=0.036) and miR-29a-3p (p=0.032) (hereafter miR-150 and miR-29a) were shown to differ significantly depending on the received RT dose in the validation cohort (Figure 3). The remaining seven candidate miRNAs identified in the screening cohort did not reach statistical significance in the validation samples (Table 3). In the validation cohort, similarly to the screening cohort, circulating levels of miR-29a and miR-150 decreased with increasing RT dose. Furthermore, miR-29a and miR-150 also significantly correlated with clinically relevant dosimetric parameters (lung mean dose; lung V20; lung V5; esophagus mean dose) that are themselves non-linearly correlated to total dose (Table 4).

Intracellular levels of miR-29a-3p and miR-150-5p increase after irradiation in NSCLC cells and in lung fibroblasts:

In all three tested NSCLC cell lines NCI-H460, A549, and NCI-H1299, radiation increased the intracellular expression of miR-29a and miR-150 as early as 2 hours after irradiation (Figure 4). This difference persisted with each fraction of radiation for up to 3 days of treatment. The same pattern of increase was also observed in two non-cancer cell lines, MRC5 and IMR90 (Figure 4). For miR-29a, the relative increase in intracellular expression peaked after the second fraction of radiation, e.g. in H1299 cells where expression returned to baseline after the third fraction. For miR-150, the relative increase in intracellular expression did not express a clear temporal trend, although expression was typically highest after the first fraction of radiation. In all experiments, miR-let-7d, miR-16-2-3p, and miR-103 demonstrated the highest Normfinder stability and were used to normalize intracellular measurements. Likewise, miR-let-7d, miR-16-2-3p, and miR-let-7a were used to normalize in exosomal measurements. In concordance with recent studies,

U6 routinely demonstrated low stability across groups, and was not used as a normalizer (44).

miR-29a-3p and miR-150-5p levels are lower in exosomes secreted into the conditioned media of cells

Western blotting confirmed the presence of TSG101 in exosome pellet samples, which were absent in the supernatant (Figure 5). miR-29a and miR-150 levels were lower in exosomes purified from conditioned media of irradiated NCI-H460, A549, and NCI-H1299 cells compared to un-irradiated control (Figure 6). This difference persisted with each fraction of radiation for up to 3 days of treatment. Exosomal miR-29a and miR-150 were also lower for irradiated MRC5 and IMR90 cells (Figure 6). At a 2Gy fractional dose, radiation treatment abrogated proliferation in all cell lines, but did not significantly induce cell death (Figure 7A). In all experiments, miR-let-7a, miR-let-7d and miR-16-2-3p demonstrated high Normfinder stability and were used to normalize exosomal miRNA measurements.

Genes predicted to be targets of miR-29a are enriched in genes that are significantly altered by radiation in H460 and H1299 cells

TargetScan identified 24 and 6 genes that are likely to be regulated by miR-29a and miR-150, respectively (Table 5). 116 studies were identified from the GEO database using the search query stated in the above methods section. Of these, 35 were relevant in terms of general experimental design. Of these, one dataset, GSE20549, included adequate descriptions of cell lines, treatment technique, and RNA extraction method. GSE20549 consisted of 42 Affymetrix microarrays (Human Exon 1.0 ST) which included 6 control replicates, 3 replicates at 2 h post-radiation, 3 replicates at 4 h post-radiation, 3 replicates at 8 h post-radiation, and 3 replicates at 24 h post-radiation for each cell line, H460 and H1299. Gene set enrichment analysis revealed that only miR-29a targets were significantly enriched in the H460 data (FDR = 0.158, Figure 8A). 6 of 24 predicted miR-29a targets (*COL1A2, COL11A1, TET3, ELN, ING3, HRK)* were significantly enriched in genes that are relatively upregulated in the non-irradiated phenotype (i.e. downregulated in the

irradiated phenotype) miR-29a targets were also relatively enriched in the H1299 data, but did not approach significance (FDR = 0.856, Figure 8B).

Discussion

The Quantitative Analyses of Normal Tissue Effects in the Clinic (QUANTEC) study delineated dosimetric parameters, such as mean lung dose (MLD) and V20, that predict RP and other endpoints of normal-tissue toxicity. Unfortunately, the constituent studies failed to identify any reliable threshold for RP. Thus, contemporary management is based on institutional and protocol guidelines for these dosimetric parameters, based on what is felt to be acceptable risk to the average patient. In principle however, even if a dosimetric threshold could be reliably established, it would only provide a population-based estimator of RP risk. What would be more clinically useful would be a constitutive biomarker that dynamically estimates risk of RP over the course of radiation therapy. Whereas dosimetry is a proxy, we wish to interrogate the biology itself.

In this study, we identified 2 miRNAs that decrease in circulation with thoracic RT in human patients with locally-advanced NSCLC. This two-miRNA signal remained significant despite inter-patient variability in our relatively small sample size, which is a limitation of our data. However, this may imply that the identified miRNAs are robust biomarkers of thoracic radiation RT, but does not preclude others that may become significant with increased statistical power. Due to institutional differences in treatment protocols, 10 of 21 patients in the validation cohort received radiation in the adjuvant setting, whereas all patients in the profiling cohort underwent definitive chemoradiotherapy. One patient in the validation cohort received no chemotherapy and the remaining patients received definitive chemoradiation. This heterogeneity in the validation cohort may have altered the rate of change in lung or tumor-specific miRNAs, as we would expect irradiated volumes to be different in the adjuvant as compared to the neoadjuvant setting. This may explain why only the two most significant signals identified in the profiling cohort remained significant in the validation cohort.

To determine the potential source of this circulating miRNA signal, we interrogated the expression of significant miRNAs intracellularly and exosomes recovered from NSCLC and stromal cell culture. To our knowledge, no prior study proposing circulating miRNAs as biomarkers for any application has identified—either *in vitro* or *ex vivo*—a validated cellular source of miRNAs. In harmony with both our screening and validation data of

miRNAs found in circulation, radiation significantly diminished miR-29a and miR-150 accumulation in exosomes secreted into conditioned media of NSCLC lines, lung fibroblasts and lung bronchoepithelial cells. This final, in vitro observation provides a second, wholly independent, confirmation that extracellular levels of miR-29a and miR-150 decrease with radiation exposure. Interestingly, whereas both miRNA biomarkers decreased *extracellularly* with radiation, they increased *intracellularly*. This inverse relationship suggests that the decrease in miR-29a and miR-150 levels in circulation may be a regulated process, rather than simply a reflection of decreasing intracellular miRNA expression. Both tumor and non-tumor cells may be downregulating the export of miRNAs, via decreased exosome secretion, leading to an intracellular buildup of miRNAs. This is further supported by our observation that a 2 Gy fraction size was sub-lethal, whereas a lysis model of miRNA release would require significant cell death (Supplemental figure S2). A conceivable alternate interpretation of the exosome expression pattern may be that radiation simply decreases cell proliferation, thereby leading to an apparent—or bulk—decrease in exosomal miRNA. This is unlikely because the significant relative decrease happens as early as 2 hrs after the first fraction of radiation, when there is a negligible difference in cell proliferation between irradiated and control samples (Figure 7B).

The decrease in exosomal export of miR-29a and miR-150 appears to hold for both NSCLC cells and lung stroma cells. While the miRNA expression patterns of other cell types found in the lung (i.e. lymphocytes and endothelial cells) were not measured, it is likely that tumor and stromal cells comprise most of the volume targeted by conformal RT methods. Another limitation of our study is the comparison between miRNA levels in circulation and miRNA levels in isolated exosomes. This comparison was necessary on a technical level because miRNAs exist in a much higher concentration in platelet-depleted plasma as compared to conditioned media. An ideal comparison would have required the isolation of exosomes from patient plasma, which we do not believe necessary due to prior studies showing that the majority of circulating miRNAs are contained within exosomes (29). These exosomes are dissolved and rendered measurable by the miRNA isolation process used in this study.

A limitation of these in-vitro data was that intracellular and exosomal miRNA expression was not measured in the same experiment. Thus, the relationship between

intracellular miRNA expression and exosomal miRNA expression is indirect. However, with the exception of larger culture plates to allow for the collection of sufficient conditioned media for exosome isolation, all other experimental conditions were identical. These data are also unable to distinguish whether the decrease in exosomal miR-29a and miR-150 is due to decreased loading of miRNAs into exosomes or due to decreased export of exosomes themselves.

Whether miRNAs circulate freely, associated with ribonucleoprotein complexes, or encapsulated within exosomes or remains to be completely elucidated (29, 52, 53). Notably, Arroyo et al. showed that miR-let-7a, miR-92a, and miR-142-3p circulate predominantly complexed to Argonaute-2 protein (a member of the RNA-induced silencing complex). Gallo et al. subsequently found that these same miRNAs, as well as all miRNAs they tested in human serum, to be much more enriched within purified exosomes. I chose to explore exosomal miRNA for two reasons. Firstly, exosome isolation allows for the concentration of extracellular miRNA, which exists at very low concentrations in conditioned media. By focusing on miRNA within the exosome fraction, which already is likely to represent most extracellular miRNA, the technical challenge of quantifying very low amounts of miRNA became tenable. Secondly, the more regulated mechanisms of miRNA trafficking within exosomes rendered this population of miRNAs more likely to be a biological response to radiation. As Gallo et al. suggests, *"Exosomal miRNA should be the starting point for early biomarker studies to reduce the probability of false negative results involving low abundance miRNAs that may be missed by using unfractionated serum or saliva."* To our knowledge, no prior study specifically shows that circulating miR-29a or miR-150 are exosome associated. However, in our data, these miRNAs had Ct values less than 35 cycles in exosome isolates but were undetectable in exosome-depleted samples.

The *post-hoc* analysis of genome data generated by an independent group in this study must be seen cautiously as preliminary results. Care was taken (see methods) to ensure that the experimental methods were well described before data were analyzed. Furthermore, a hypothesis (that genes regulated by miRNA observed to be radiation-responsive would also be significant in changes in gene expression in irradiated cells) was the focus for the GSEA analyses undertaken in this study, rather than a random, catch-all, of many disparate biological pathways.

Gene set enrichment analysis revealed that miR-29a may play an important role in tumor cell's response to radiation. In H460 cells, 6 genes that are predicted to be regulated by miR-29a are upregulated in non-irradiated cells as compared to irradiated cells. Because miRNAs are known to repress gene expression, this is in concordance with the relative increase in intracellular miR-29a observed with radiation. Interestingly, 3 of these (*COL1A2, COL11A1,* and *ELN)* belong to a family of extracellular matrix proteins and another (*ING3)* plays a part in macrophage activation. No conclusions can be drawn based on the analyses of gene expression in H1299 cells since neither gene sets approached significance. Many other gene sets were available for analysis, but were not specifically relevant to miRNA expression, and were thus beyond the scope of this study.

Our results concur with previous studies by Templin and colleagues showing a significant decrease of miR-150 in the blood of mice exposed to whole body radiation (25). Our laboratory has also found that miR-150 decreases in the circulation of mice exposed specifically to thoracic radiation (unpublished data). miR-150 has been identified as an important promotor of inflammation via its regulation of MYB, which is itself a conserved regulator of hematopoiesis (54, 55). Adams and colleagues demonstrated that over-expression of miR-150 impaired bone marrow reconstitution after hematopoietic ablation with 5-flourouracil (56). In the context of circulating miRNAs, miR-150 may be a general marker of a leukocyte-driven inflammatory response in mammals exposed to ionizing radiation. In contrast, there has been no prior study linking miR-29a to radiation response. miR-29a is known to be highly expressed in the mammalian lung, heart, and kidney (57-59). It is well described as an inhibitor of extracellular matrix (ECM) remodeling via its binding of 21 downstream proteins in the TGF-β/Smad3 pathway. Reduction in miR-29a levels has been associated with bleomycin-induced lung fibrosis (58), myocardial fibrosis after ischemia (57), and renal fibrosis in hypertensive disease (59). The decrease in circulating levels of miR-29a after thoracic radiation may thus be related to a pro-fibrotic state. Alternatively, the concomitant increase in intracellular miR-29a may be an adaptive response to radiation exposure. This has direct implications for miR-29a being a specific biomarker of interest for predicting radiation pneumonitis. Indeed, miR-29a had significantly higher statistical correlation with radiation dose compared to miR-150 in patients undergoing thoracic RT. Furthermore, data from the Cancer Genome Atlas also

reveals that miR-29a is expressed at much higher levels in both NSCLC tumors and normal lung tissue compared to miR-150 (Figure 9).

Conclusion and Future Directions

In conclusion, we show from an unbiased screen that miR-29a and miR-150 decrease in the circulation of NSCLC patients undergoing thoracic RT. Furthermore, this miRNA signal may originate—at least in part—from intracellular accumulation and concomitant reduction in exosome export from NSCLC and stromal cells. While miR-150 is likely a general biomarker of any tissue exposed to radiation, the reduction in circulating miR-29a may reflect a pro-fibrotic or adaptive state in the lung specifically. Patients whose levels of miR-29a decrease significantly more (in a pro-fibrosis model), or less (in an adaptive model), compared to average may be at higher risk for normal tissue toxicity, regardless of their estimated lung V5, lung V20, or lung MLD. Likewise, these differential expression patterns may reflect biological tumor response (or resistance) to radiation.

The successful translation of this present work depends upon correlating trends in circulating miR-29a and miR-150 expression with clinical endpoints such as late effects, tumor response, or even mortality. A larger patient population will be required to statistically power such a future study, as the primary endpoint of interest—radiation pneumonitis—occurs in only 5-20% of patients. This present work has formed the basis for recruiting additional patients at the Dana Farber Cancer Institute (DFCI). As of the submission of this thesis, serial blood samples from 15 patients undergoing definitive radiation therapy for NSCLC have been collected. Because the in-vitro data showed that non-tumor cells also express the decrease in circulating radiation-responsive miRNAs, this biomarker may conceivably correspond more to normal tissue toxicity rather than tumor response. As such, this biomarker signature may be also useful for estimating risk of normal tissue toxicity in patients with lung cancers other than Stage IIIA. This would include the increasing number of patients with early, Stage I tumors that are being detected due to routine screening in elderly smokers (60). Interestingly, these patients do not undergo multi-week courses of fractionated radiation therapy, but more often single courses of ablative stereotactic body radiation therapy (SBRT). In this context, miRNA biomarkers may be helpful in predicting those who need close monitoring for radiation-induced pneumonitis rather than for dose-reduction.

A challenge in this future study is the relatively long follow-up time required to accrue late effects endpoints (RP can be observed up to one year after the completion of RT). Nonetheless, the strength of these potential biomarkers is that they can be collected and measured with ease and at very low cost. A near-term goal of this work is to establish a normative curve of circulating miRNA expression in patients who do not experience late effects from which outlier expression trends would predict toxicity. Alternatively, miRNA biomarkers may predict radiation resistance and tumor response (Figure 10). There is no guarantee that miR-29a and miR-150 are actually biomarkers of either effect. However, we posit that if any such useful biomarker exists, it is likely to first trend with exposure to thoracic radiation. That is, a biomarker of any particular radiation effect must first be radiation-responsive. In narrowing thousands of miRNAs that can be found in circulation down to two that correlate with radiation exposure, this work lays the foundation for identifying clinically useful biomarkers of radiation treatment. Such a tool would powerfully advance the goal of tailoring radiation therapy to each patient's biology in real time.

There are likely limits to using biomarkers of normal-tissue toxicity to adjust radiation dose. In two prospective, randomized trials of 551 patients with lung cancer, 40 Gy regimens of RT were significantly inferior to 60 Gy regimens for local control (61). Thus, even if a patient were predicted to have pulmonary toxicity due to radiation therapy, that tradeoff may still be acceptable for adequate tumor control. What is more likely to be useful should miR-29a and miR-150 be reliable biomarkers of toxicity is informing dose-escalation. A conceivable prospective trial to test the clinical utility of such biomarkers would be to measure these markers in all patients getting standard RT for NSCLC up to 60 Gy. Patients with outlier trends in these markers (predicting toxicity) would only receive 60 Gy while those with normal trends (predicting no toxicity) would be randomized to either 60 Gy or dose-escalation to 70 Gy. This would be a better design than the TGF-beta-guided dose-escalation trial attempted by Anscher and colleagues because it would allow for comparing standard versus higher dose treatments in patients who are predicted to have less toxicity (15).

Beyond adjustment of radiation dose, circulating miRNAs may give information concerning the biological changes in the body due to treatment, and provide a basis for

intervention. For example, because a decrease in circulating miR-29a may herald a TGF-β mediated pro-fibrotic state in the lung, patients shown to have exaggerated declines in miR-29a levels may be candidates for anti-TGF-β therapy. The monoclonal antibody against TGF-β, Fresolimumab, has already been shown to have safety and activity in humans (62). However, the potential for using biomarkers to drive biologic intervention must be accompanied by a consideration of the high cost of such therapies. Biologics—specifically monoclonal antibodies—are among the most expensive pharmaceuticals and contribute to the incessantly rising cost of healthcare in the United States (63). It is evident that, even if Fresolimumab were effective in preventing radiation pneumonitis, it should only be offered to a small subset of patients who are most at risk for severe toxicity. Circulating miRNAs that can be collected and measured at very low cost can be extremely useful in identifying this population of patients. This degree of biological precision would lead not only to clinical benefits, but also economic savings.

The general approach of measuring circulating miRNAs to identify potential biomarkers can also be extended to other disease sites. While miR-29a may be a lung-specific marker, miRNA profiling could potentially identify other organ-specific miRNAs that are radiation-responsive. Supported by the preliminary data in this study, patients undergoing RT for prostate cancer at the DFCI will be enrolled in a pilot study in which circulating miRNAs will be profiled for potential biomarkers of radiation-induced proctitis. Similarly, this approach can be applied to any disease site where radiation therapy is standard of care and there is high concern for normal-tissue toxicity such as for breast (brachial plexopathy) and for pancreas (enteritis).

Summary

Radiation therapy (RT) is an important part of standard treatment for lung cancer. The benefits of RT must be carefully weighed by the risks of radiation toxicity to normal lung tissue that exists in intimate proximity to tumor. The goal of this study is to find an early marker of radiation exposure that can be measured in the blood of patients undergoing RT. This marker of radiation exposure—or biomarker—may be useful to predict eventual toxicity or disease response to radiation before they occur. This technology would allow clinicians to make adjustments to treatment plans in order to prevent or treat toxicities that would otherwise damage structures such as the lungs or esophagus. Micro-RNAs (miRNAs) are small nucleic acids that regulate many genes in the human body. In the blood, they are remarkably stable and diverse, making them good candidates to be biomarkers for RT. In this study, 1900 miRNAs were measured in the blood of 5 patients undergoing RT for lung cancer. 10 miRNAs were found to correspond with increasing doses of radiation that patients receive over their 6 to 7 week treatment course. To validate this correlation, these 10 miRNA signatures were specifically measured in the blood of an independent set of 21 lung cancer patients. 2 miRNAs, miR-29a-3p and miR-150-5p, remained significant in this validation group. Experiments were also conducted on lung cancer cells previously isolated from a single tumor as well as normal cells. When these cells were treated with radiation, the levels of miR-29a and miR-150 measured within them increased, while the levels of these miRNAs in their environment decreased. Together, these data suggests that both tumor and normal cells decrease the export of miR-29a and miR-150 in a regulated manner, making them attractive candidates as biomarkers for radiation response. By measuring trends in miR-29a and miR-150 in the blood of patients undergoing RT, clinicians may be able to predict toxicity, and therefore tailor care precisely to that patient's unique biology.

Contributions

Khang Dinh, the author, performed all experiments, data analysis, and drafting of this thesis. Wocjiech Fendler is a biostatistician who was instrumental to the analysis of profiling data and provided statistical methods. Colin O'Leary and Peter Deraska contributed to cell culture experiments and figure formatting. Sanket Acharya and Dipanjan Chowdhury provided technical miRNA guidance. David Kozono and Alan D'Andrea were responsible for the project conception, some experimental designs, and data interpretation.

Works Cited

1. Siegel RL, Miller KD, Jemal A. Cancer statistics, 2015. CA: a cancer journal for clinicians. 2015;65(1):5-29. Epub 2015/01/07. doi: 10.3322/caac.21254. PubMed PMID: 25559415.
2. Molina JR, Yang P, Cassivi SD, Schild SE, Adjei AA, editors. Non-small cell lung cancer: epidemiology, risk factors, treatment, and survivorship. Mayo Clinic Proceedings; 2008: Elsevier.
3. Ramnath N, Dilling TJ, Harris LJ, Kim AW, Michaud GC, Balekian AA, et al. CHEST Supplement. Chest. 2013;143(5):e314S-e40S.
4. Garg S, Gielda BT, Kiel K, Turian JV, Fidler MJ, Batus M, et al. Patterns of locoregional failure in stage III non-small cell lung cancer treated with definitive chemoradiation therapy. Practical radiation oncology. 2014;4(5):342-8. doi: 10.1016/j.prro.2013.12.002. PubMed PMID: 25194104.
5. van Meerbeeck JP, Kramer GWPM, Van Schil PEY, Legrand C, Smit EF, Schramel F, et al. Randomized Controlled Trial of Resection Versus Radiotherapy After Induction Chemotherapy in Stage IIIA-N2 Non–Small-Cell Lung Cancer. Journal of the National Cancer Institute. 2007;99(6):442-50. doi: 10.1093/jnci/djk093.
6. Albain KS, Swann RS, Rusch VW, Turrisi AT, Shepherd FA, Smith C, et al. Radiotherapy plus chemotherapy with or without surgical resection for stage III non-small-cell lung cancer: a phase III randomised controlled trial. The Lancet. 2009;374(9687):379-86.
7. Bradley JD, Paulus R, Komaki R, Masters G, Blumenschein G, Schild S, et al. Standard-dose versus high-dose conformal radiotherapy with concurrent and consolidation carboplatin plus paclitaxel with or without cetuximab for patients with stage IIIA or IIIB non-small-cell lung cancer (RTOG 0617): a randomised, two-by-two factorial phase 3 study. The Lancet Oncology. 2015;16(2):187-99. doi: 10.1016/S1470-2045(14)71207-0. PubMed PMID: 25601342; PubMed Central PMCID: PMC4419359.
8. Marks LB, Bentzen SM, Deasy JO, Kong FM, Bradley JD, Vogelius IS, et al. Radiation dose-volume effects in the lung. International journal of radiation oncology, biology, physics. 2010;76(3 Suppl):S70-6. Epub 2010/03/05. doi: 10.1016/j.ijrobp.2009.06.091. PubMed PMID: 20171521; PubMed Central PMCID: PMCPMC3576042.
9. Mehta V. Radiation pneumonitis and pulmonary fibrosis in non–small-cell lung cancer: Pulmonary function, prediction, and prevention. International Journal of Radiation Oncology* Biology* Physics. 2005;63(1):5-24.
10. Jenkins P, D'Amico K, Benstead K, Elyan S. Radiation pneumonitis following treatment of non–small-cell lung cancer with continuous hyperfractionated accelerated radiotherapy (CHART). International Journal of Radiation Oncology* Biology* Physics. 2003;56(2):360-6.
11. Bentzen SM, Parliament M, Deasy JO, Dicker A, Curran WJ, Williams JP, et al. Biomarkers and surrogate endpoints for normal-tissue effects of radiation therapy: the importance of dose–volume effects. International Journal of Radiation Oncology* Biology* Physics. 2010;76(3):S145-S50.
12. Li C, Wilson PB, Levine E, Barber J, Stewart AL, Kumar S. TGF-β1 levels in pre-treatment plasma identify breast cancer patients at risk of developing post-radiotherapy fibrosis. International journal of cancer. 1999;84(2):155-9.
13. Anscher MS, Kong F-M, Andrews K, Clough R, Marks LB, Bentel G, et al. Plasma transforming growth factor β1 as a predictor of radiation pneumonitis. International Journal of Radiation Oncology* Biology* Physics. 1998;41(5):1029-35.
14. Zhao L, Wang L, Ji W, Wang X, Zhu X, Hayman JA, et al. Elevation of plasma TGF-β1 during radiation therapy predicts radiation-induced lung toxicity in patients with non-small-cell lung cancer: a combined analysis from Beijing and Michigan. International Journal of Radiation Oncology* Biology* Physics. 2009;74(5):1385-90.

15. Anscher MS, Marks LB, Shafman TD, Clough R, Huang H, Tisch A, et al. Risk of long-term complications after TFG-β1–guided very-high-dose thoracic radiotherapy. International Journal of Radiation Oncology* Biology* Physics. 2003;56(4):988-95.
16. Novakova-Jiresova A, van Gameren MM, Coppes RP, Kampinga HH, Groen HJ. Transforming growth factor-β plasma dynamics and post-irradiation lung injury in lung cancer patients. Radiotherapy and oncology. 2004;71(2):183-9.
17. Evans ES, Kocak Z, Zhou S-M, Kahn DA, Huang H, Hollis DR, et al. Does transforming growth factor-β1 predict for radiation-induced pneumonitis in patients treated for lung cancer? Cytokine. 2006;35(3):186-92.
18. Chen Y, Rubin P, Williams J, Hernady E, Smudzin T, Okunieff P. Circulating IL-6 as a predictor of radiation pneumonitis. International Journal of Radiation Oncology* Biology* Physics. 2001;49(3):641-8.
19. Chen Y, Hyrien O, Williams J, Okunieff P, Smudzin T, Rubin P. Interleukin (IL)-1A and IL-6: applications to the predictive diagnostic testing of radiation pneumonitis. International Journal of Radiation Oncology* Biology* Physics. 2005;62(1):260-6.
20. Stenmark MH, Cai X-W, Shedden K, Hayman JA, Yuan S, Ritter T, et al. Combining physical and biologic parameters to predict radiation-induced lung toxicity in patients with non-small-cell lung cancer treated with definitive radiation therapy. International Journal of Radiation Oncology* Biology* Physics. 2012;84(2):e217-e22.
21. Chen X, Ba Y, Ma L, Cai X, Yin Y, Wang K, et al. Characterization of microRNAs in serum: a novel class of biomarkers for diagnosis of cancer and other diseases. Cell research. 2008;18(10):997-1006.
22. Bartel DP. MicroRNAs: genomics, biogenesis, mechanism, and function. cell. 2004;116(2):281-97.
23. Bartel DP. MicroRNAs: target recognition and regulatory functions. Cell. 2009;136(2):215-33.
24. Guo H, Ingolia NT, Weissman JS, Bartel DP. Mammalian microRNAs predominantly act to decrease target mRNA levels. Nature. 2010;466(7308):835-40.
25. Templin T, Amundson SA, Brenner DJ, Smilenov LB. Whole mouse blood microRNA as biomarkers for exposure to &b. gamma;-rays and 56Fe ions. International journal of radiation biology. 2011;87(7):653-62.
26. Cui W, Ma J, Wang Y, Biswal S. Plasma miRNA as biomarkers for assessment of total-body radiation exposure dosimetry. PloS one. 2011;6(8):e22988.
27. Templin T, Paul S, Amundson SA, Young EF, Barker CA, Wolden SL, et al. Radiation-induced micro-RNA expression changes in peripheral blood cells of radiotherapy patients. International Journal of Radiation Oncology* Biology* Physics. 2011;80(2):549-57.
28. Chowdhury D, Choi YE, Brault ME. Charity begins at home: non-coding RNA functions in DNA repair. Nature Reviews Molecular Cell Biology. 2013;14(3):181-9.
29. Gallo A, Tandon M, Alevizos I, Illei GG. The majority of microRNAs detectable in serum and saliva is concentrated in exosomes. PloS one. 2012;7(3):e30679.
30. Chen X, Liang H, Zhang J, Zen K, Zhang C-Y. Secreted microRNAs: a new form of intercellular communication. Trends in cell biology. 2012;22(3):125-32.
31. Valadi H, Ekström K, Bossios A, Sjöstrand M, Lee JJ, Lötvall JO. Exosome-mediated transfer of mRNAs and microRNAs is a novel mechanism of genetic exchange between cells. Nature cell biology. 2007;9(6):654-9.
32. Mittelbrunn M, Gutiérrez-Vázquez C, Villarroya-Beltri C, González S, Sánchez-Cabo F, González MÁ, et al. Unidirectional transfer of microRNA-loaded exosomes from T cells to antigen-presenting cells. Nature communications. 2011;2:282.
33. Pegtel DM, Cosmopoulos K, Thorley-Lawson DA, van Eijndhoven MA, Hopmans ES, Lindenberg JL, et al. Functional delivery of viral miRNAs via exosomes. Proceedings of the National Academy of Sciences. 2010;107(14):6328-33.

34. Agarwal V, Bell GW, Nam J-W, Bartel DP. Predicting effective microRNA target sites in mammalian mRNAs. eLife. 2015;4. doi: 10.7554/eLife.05005.
35. Lewis BP, Burge CB, Bartel DP. Conserved seed pairing, often flanked by adenosines, indicates that thousands of human genes are microRNA targets. Cell. 2005;120(1):15-20. Epub 2005/01/18. doi: 10.1016/j.cell.2004.12.035. PubMed PMID: 15652477.
36. Carney DN, Gazdar AF, Bepler G, Guccion JG, Marangos PJ, Moody TW, et al. Establishment and identification of small cell lung cancer cell lines having classic and variant features. Cancer research. 1985;45(6):2913-23.
37. Lieber M, Todaro G, Smith B, Szakal A, Nelson-Rees W. A continuous tumor-cell line from a human lung carcinoma with properties of type II alveolar epithelial cells. International Journal of Cancer. 1976;17(1):62-70.
38. Phelps RM, Johnson BE, Ihde DC, Gazdar AF, Carbone DP, McClintock PR, et al. NCI-navy medical oncology branch cell line data base. Journal of cellular biochemistry. 1996;63(S24):32-91.
39. Jacobs JP, Jones CM, Baille JP. Characteristics of a human diploid cell designated MRC-5. Nature. 1970;227(5254):168-70. Epub 1970/07/11. PubMed PMID: 4316953.
40. Nichols W, Murphy D, Cristofalo V, Toji L, Greene A, Dwight S. Characterization of a new human diploid cell strain, IMR-90. Science. 1977;196(4285):60-3.
41. Eldh M, Lötvall J, Malmhäll C, Ekström K. Importance of RNA isolation methods for analysis of exosomal RNA: evaluation of different methods. Molecular immunology. 2012;50(4):278-86.
42. Schmittgen TD, Livak KJ. Analyzing real-time PCR data by the comparative C(T) method. Nature protocols. 2008;3(6):1101-8. Epub 2008/06/13. PubMed PMID: 18546601.
43. Strober W. Trypan blue exclusion test of cell viability. Current protocols in immunology. 2001:A. 3B. 1-A. 3B. 2.
44. Peltier HJ, Latham GJ. Normalization of microRNA expression levels in quantitative RT-PCR assays: Identification of suitable reference RNA targets in normal and cancerous human solid tissues. Rna. 2008;14(5):844-52.
45. Acharya SS, Fendler W, Watson J, Hamilton A, Pan Y, Gaudiano E, et al. Serum microRNAs are early indicators of survival after radiation-induced hematopoietic injury. Science translational medicine. 2015;7(287):287ra69-ra69.
46. Andersen CL, Jensen JL, Orntoft TF. Normalization of real-time quantitative reverse transcription-PCR data: a model-based variance estimation approach to identify genes suited for normalization, applied to bladder and colon cancer data sets. Cancer Res. 2004;64(15):5245-50. Epub 2004/08/04. doi: 10.1158/0008-5472.can-04-0496. PubMed PMID: 15289330.
47. Li Y, Zhang L, Liu F, Xiang G, Jiang D, Pu X. Identification of endogenous controls for analyzing serum exosomal miRNA in patients with hepatitis B or hepatocellular carcinoma. Disease markers. 2015;2015:893594. Epub 2015/03/31. doi: 10.1155/2015/893594. PubMed PMID: 25814782; PubMed Central PMCID: PMCPMC4357047.
48. Blondal T, Nielsen SJ, Baker A, Andreasen D, Mouritzen P, Teilum MW, et al. Assessing sample and miRNA profile quality in serum and plasma or other biofluids. Methods. 2013;59(1):S1-S6.
49. Mootha VK, Lindgren CM, Eriksson K-F, Subramanian A, Sihag S, Lehar J, et al. PGC-1α-responsive genes involved in oxidative phosphorylation are coordinately downregulated in human diabetes. Nature genetics. 2003;34(3):267-73.
50. Subramanian A, Tamayo P, Mootha VK, Mukherjee S, Ebert BL, Gillette MA, et al. Gene set enrichment analysis: A knowledge-based approach for interpreting genome-wide expression profiles. Proceedings of the National Academy of Sciences. 2005;102(43):15545-50. doi: 10.1073/pnas.0506580102.
51. Benjamini Y, Hochberg Y. Controlling the false discovery rate: a practical and powerful approach to multiple testing. Journal of the Royal Statistical Society Series B (Methodological). 1995:289-300.

52. Turchinovich A, Weiz L, Langheinz A, Burwinkel B. Characterization of extracellular circulating microRNA. Nucleic acids research. 2011:gkr254.
53. Arroyo JD, Chevillet JR, Kroh EM, Ruf IK, Pritchard CC, Gibson DF, et al. Argonaute2 complexes carry a population of circulating microRNAs independent of vesicles in human plasma. Proceedings of the National Academy of Sciences. 2011;108(12):5003-8.
54. Xiao C, Calado DP, Galler G, Thai TH, Patterson HC, Wang J, et al. MiR-150 controls B cell differentiation by targeting the transcription factor c-Myb. Cell. 2007;131(1):146-59. Epub 2007/10/10. doi: 10.1016/j.cell.2007.07.021. PubMed PMID: 17923094.
55. Lin YC, Kuo MW, Yu J, Kuo HH, Lin RJ, Lo WL, et al. c-Myb is an evolutionary conserved miR-150 target and miR-150/c-Myb interaction is important for embryonic development. Molecular biology and evolution. 2008;25(10):2189-98. Epub 2008/08/01. doi: 10.1093/molbev/msn165. PubMed PMID: 18667440.
56. Adams BD, Guo S, Bai H, Guo Y, Megyola CM, Cheng J, et al. An in vivo functional screen uncovers miR-150-mediated regulation of hematopoietic injury response. Cell reports. 2012;2(4):1048-60. Epub 2012/10/23. doi: 10.1016/j.celrep.2012.09.014. PubMed PMID: 23084747; PubMed Central PMCID: PMCPMC3487471.
57. van Rooij E, Sutherland LB, Thatcher JE, DiMaio JM, Naseem RH, Marshall WS, et al. Dysregulation of microRNAs after myocardial infarction reveals a role of miR-29 in cardiac fibrosis. Proceedings of the National Academy of Sciences of the United States of America. 2008;105(35):13027-32. Epub 2008/08/30. doi: 10.1073/pnas.0805038105. PubMed PMID: 18723672; PubMed Central PMCID: PMCPMC2529064.
58. Xiao J, Meng XM, Huang XR, Chung AC, Feng YL, Hui DS, et al. miR-29 inhibits bleomycin-induced pulmonary fibrosis in mice. Molecular therapy : the journal of the American Society of Gene Therapy. 2012;20(6):1251-60. Epub 2012/03/08. doi: 10.1038/mt.2012.36. PubMed PMID: 22395530; PubMed Central PMCID: PMCPMC3369297.
59. Qin W, Chung AC, Huang XR, Meng XM, Hui DS, Yu CM, et al. TGF-beta/Smad3 signaling promotes renal fibrosis by inhibiting miR-29. Journal of the American Society of Nephrology : JASN. 2011;22(8):1462-74. Epub 2011/07/26. doi: 10.1681/asn.2010121308. PubMed PMID: 21784902; PubMed Central PMCID: PMCPMC3148701.
60. Team NLSTR. Reduced lung-cancer mortality with low-dose computed tomographic screening. The New England journal of medicine. 2011;365(5):395.
61. Perez CA, Pajak TF, Rubin P, Simpson JR, Mohiuddin M, Brady LW, et al. Long-term observations of the patterns of failure in patients with unresectable non-oat cell carcinoma of the lung treated with definitive radiotherapy report by the radiation therapy oncology group. Cancer. 1987;59(11):1874-81.
62. Trachtman H, Fervenza FC, Gipson DS, Heering P, Jayne DR, Peters H, et al. A phase 1, single-dose study of fresolimumab, an anti-TGF-β antibody, in treatment-resistant primary focal segmental glomerulosclerosis. Kidney international. 2011;79(11):1236-43.
63. Engelberg AB, Kesselheim AS, Avorn J. Balancing innovation, access, and profits—market exclusivity for biologics. New England Journal of Medicine. 2009;361(20):1917-9.

Tables

Table 1. Patient characteristics of profiling cohort. Abbreviations: SCC, squamous cell carcinoma; AC, adenocarcinoma

Patient	Age	Gender	Diagnosis	Chemotherapy	RT Dose
2468	76	F	Stage IIIA SCC	Carboplatin + Taxol	60 Gy
2510	61	F	Stage IIIA Adenocarcinoma	Cisplatin + Etoposide	66 Gy
2526	60	M	Stage IIIA Adenocarcinoma	Cisplatin + Etoposide	54 Gy
2534	60	F	Stage IIIA SCC	Cisplatin + Etoposide	66 Gy
2561	67	M	Stage IIIA Adenocarcinoma	Carboplatin + Taxol	66 Gy

Table 2. Patient characteristics of validation cohort. Abbreviations: R1, positive microscopic margins; R2, positive gross margins; SCC, squamous cell carcinoma; PN, cisplatin/navelbine; KG, carboplatin/gemcitabine; PG, cisplatin/gemcitabine; KN, carboplatin/navelbine; NOT*, not otherwise specified

Patient	Age	Gender	Diagnosis	Indication	Chemotherapy	RT Dose
AE1	58	F	IIA SSC	Recurrence/adjuvant	PN	70 Gy
BE1	68	M	IIIA SSC	Definitive	KG	66 Gy
CG1	55	M	IIA SSC	R2/adjuvant	PN	68 Gy
DW1	59	F	IIB SSC	R1/adjuvant	PN	68 Gy
FL1	76	M	IIIA SSC	Definitive	PG	66 Gy
GH1	62	F	IIIB SCC	Definitive	PN	66 Gy
GK1	67	M	IIIB SSC	Definitive	KN	66 Gy
KA1	64	F	IIIB Adenocarcinoma	Definitive	PN	58 Gy
KA2	64	M	IIB SSC	R1/adjuvant	PN	60 Gy
KI1	68	F	IIIA SSC	R1/adjuvant	KN	60 Gy
LM1	67	M	IIIA SSC	R1/adjuvant	PN	60 Gy
LJ1	77	M	IIIA SSC	R1/adjuvant	No Chemotherapy	56 Gy
MS1	70	M	IIIA SSC	R1/adjuvant	KN	66 Gy
PB1	60	M	IIIA	Definitive	PG	64 Gy
SJ1	55	M	IIB	R1/adjuvant	PN	66 Gy
SW1	62	M	IIIB Adenocarcinoma	Definitive	PN	66 Gy
WJ1	73	M	IIIA Adenocarcinoma	Definitive	PG	60 Gy
ZA1	78	M	IIIA Adenocarcinoma	Definitive	KG	66 Gy

Table 3. Validation of miRNAs candidates. Average dCp values with standard deviation at 0, 20, and 40 Gy timepoints are shown for each miRNA identified in the profiling cohort. P-values were calculated as described in the methods section. Only miR-29a and miR-150 showed statistically significant correlation with RT dose in the validation cohort of 21 patients.

miRNA	0 Gy	20 Gy	40 Gy	p-value
miR-29a-3p	1.16 ± 1.09	0.43 ± 0.65	0.67 ± 1.25	0.0203
miR-150-5p	2.91 ± 1.34	1.98 ± 1.17	1.92 ± 1.49	0.0298
miR-101-5p	-1.12 ± 1.25	-2.02 ± 1.57	-0.99 ± 1.21	0.1262
miR-342-3p	1.83 ± 0.99	1.15 ± 1.00	1.23 ± 1.35	0.1383
miR-30d-5p	2.76 ± 1.06	2.57 ± 1.56	2.69 ± 1.72	0.9153
miR-320a	4.24 ± 0.93	4.09 ± 1.04	3.94 ± 1.36	0.5670
miR-142-3p	4.84 ± 1.18	4.68 ± 0.90	4.78 ± 1.16	0.8968
miR-191-5p	2.73 ± 0.87	2.55 ± 1.08	2.69 ± 1.54	0.8666
miR-125p-5p	1.21 ± 1.05	0.98 ± 0.75	1.21 ± 1.19	0.8222
miR-15b-5p	2.94 ± 1.30	2.85 ± 1.21	2.87 ± 1.21	0.9561

Table 4. Of 10 miRNAs significantly correlated with total dose, 7 are also significantly correlated with lung V20, MLD, lung V5, or esophagus mean dose. Pearson correlation coefficient (R) and p-values are reported.

Correlation of miRNA expression to computed dosimetric parameters

		miR-29a-3p	miR-150-5p	miR-101-5p	miR-342-3p	miR-30d-5p	miR-320a	miR-142-3p	miR-191-5p	miR-125b-5p	miR-15b-5p
Lung V20	R:	-0.63	-0.54	0.50	-0.39	-0.08	0.06	-0.36	0.44	-0.32	0.49
	p:	0.003	0.014	0.029	0.086	0.748	0.811	0.120	0.052	0.174	0.030
MLD	R:	-0.71	-0.62	0.57	-0.53	0.04	0.19	-0.43	0.54	-0.43	0.60
	p:	0.001	0.003	0.011	0.017	0.862	0.415	0.059	0.015	0.058	0.005
Lung V5	R:	-0.61	-0.55	0.45	-0.40	-0.05	0.23	-0.50	0.43	-0.22	0.50
	p:	0.005	0.012	0.053	0.082	0.821	0.331	0.024	0.060	0.356	0.024
EsoMean	R:	-0.71	-0.70	0.54	-0.51	0.14	0.23	-0.50	0.55	-0.43	0.54
	p:	<0.001	0.001	0.017	0.020	0.547	0.328	0.026	0.013	0.057	0.013

Table 5. Predicted gene targets of miR-29a (left) and miR-150 (right) by TargetScan. 6 of 24 genes predicted to be regulated by miR-29a are enriched in genes whose expression is downregulated in H460 cells exposed to radiation.

Predicted miR-29a-3p Targets		
Gene	**Protein Name**	**Enriched**
COL1A1	collagen, type I, alpha 1	No
TET3	tet methylcytosine dioxygenase 3	Yes
TET1	tet methylcytosine dioxygenase 1	No
PI15	peptidase inhibitor 15	No
TET2	tet methylcytosine dioxygenase 2	No
ATAD2B	ATPase family, AAA domain containing 2B	No
HRK	harakiri, BCL2 interacting protein (contains only BH3 domain)	Yes
COL3A1	collagen, type III, alpha 1	No
ELN	elastin	Yes
ING3	inhibitor of growth family, member 3	Yes
TRIB2	tribbles pseudokinase 2	No
SUV420H2	suppressor of variegation 4-20 homolog 2 (Drosophila)	No
XKR6	XK, Kell blood group complex subunit-related family, member 6	No
COL1A2	collagen, type I, alpha 2	Yes
NFIA	nuclear factor I/A	No
EIF4E2	eukaryotic translation initiation factor 4E family member 2	No
TIMM8B	translocase of inner mitochondrial membrane 8 homolog B (yeast)	No
HBP1	HMG-box transcription factor 1	No
TDG	thymine-DNA glycosylase	No
IFI30	interferon, gamma-inducible protein 30	No
C1orf220	chromosome 1 open reading frame 220	No
COL11A1	collagen, type XI, alpha 1	Yes
C1QTNF6	C1q and tumor necrosis factor related protein 6	No
ADAMTS9	ADAM metallopeptidase with thrombospondin type 1 motif, 9	No

Predicted miR-150-5p Targets		
Gene	**Protein Name**	**Enriched**
SLC35E3	solute carrier family 35, member E3	No
MYB	v-myb avian myeloblastosis viral oncogene homolog	No
MDM4	Mdm4 p53 binding protein homolog (mouse)	No
FAM83F	family with sequence similarity 83, member F	No
ENSA	endosulfine alpha	No
C5orf58	chromosome 5 open reading frame 58	No

Figures

Figure 1. Background expression of miRNAs. Expression of miR-29a and miR-150 is substantially higher in exosomes isolated from cell-conditioned media compared to exosomes isolated from cellfree, FBS-containing media. Levels are reported as relative fold difference and normalized to conditioned media. Notably, miR-150 was undetectable in cell-free media and Ct values of 40 (upper limit) were assigned for comparison, leading to the >400 fold difference in some cultured media samples.

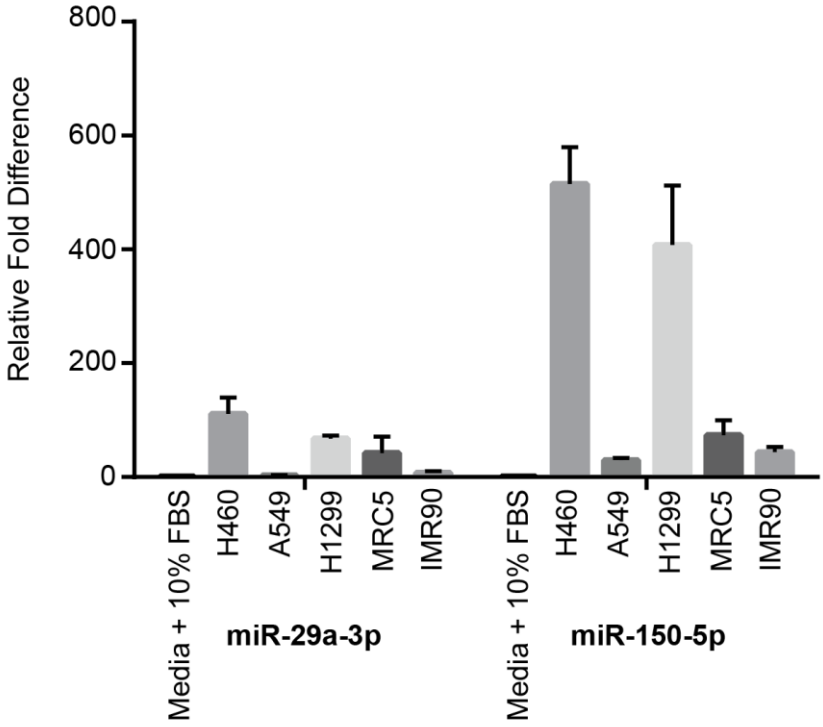

Figure 2. Heatmap of statistically significant signatures from a miRNA screen of patient blood samples taken over six weeks of radiation therapy. Of 124 universally expressed miRNAs, 10 were significantly correlated with RT dose. Five miRNAs decreased in expression in circulation with increasing radiation dose while five increased in expression. ANOVA p-values are reported.

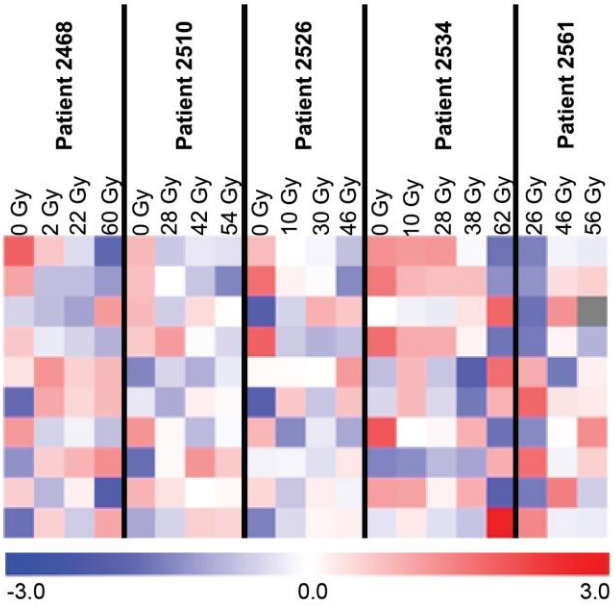

miRNA	p-value	Relative Fold Change
miR-29a-3p	0.0037	0.47 (down)
miR-150-5p	0.0083	0.16 (down)
miR-101-5p	0.0140	3.36 (up)
miR-342-3p	0.0173	0.56 (down)
miR30d-5p	0.0210	1.34 (up)
miR-320a	0.0252	1.13 (up)
miR-142-3p	0.0291	0.46 (down)
miR191-5p	0.0352	2.06 (up)
miR-125b-5p	0.0450	0.65 (down)
miR-15b-5p	0.0484	1.77 (up)

Figure 3. (A) miR-29a-3p and (B) miR-150-5p expression significantly decreased in the circulation of patients undergoing thoracic RT in the validation cohort (overall p = 0.020 and 0.030, respectively). P-values displayed are post-hoc comparisons between 0 and 20 Gy, 20 and 40 Gy, and 0 and 40 Gy. Higher dCp scores represent higher expression levels. Error bars represent standard deviation.

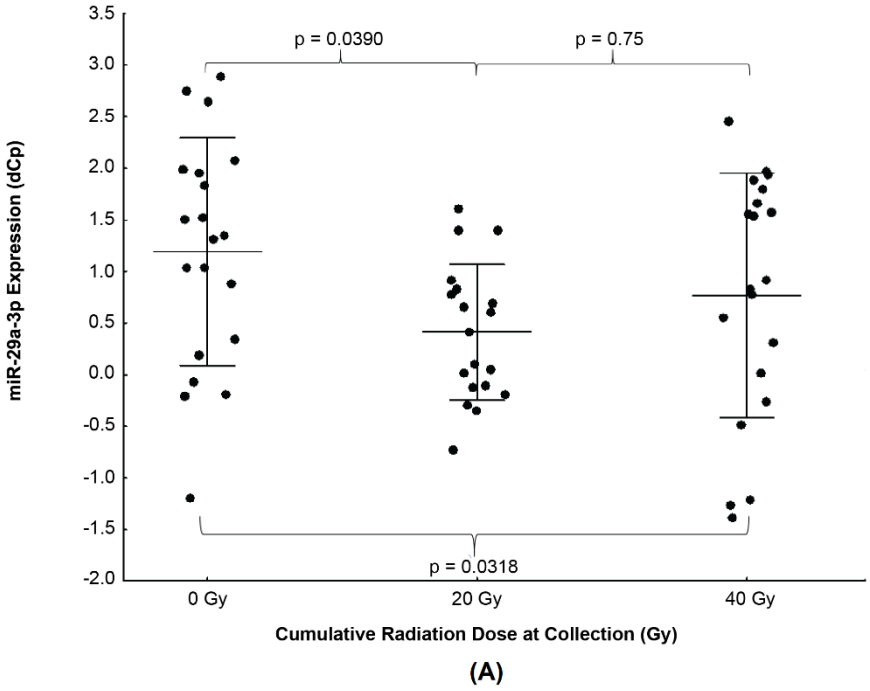

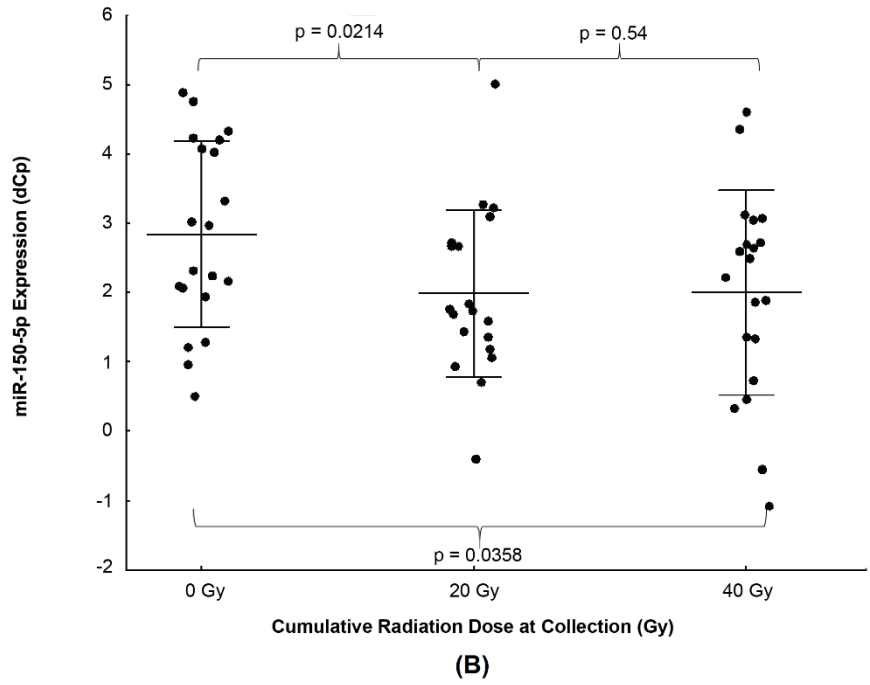

Figure 4. Intracellular expression of miR-29a and miR-150 increased with radiation in both NSCLC and stromal cell lines after 1, 2 or 3 days of 2 Gy fractions. Error bars represent standard deviation (*p < 0.05, ***p < 0.001).

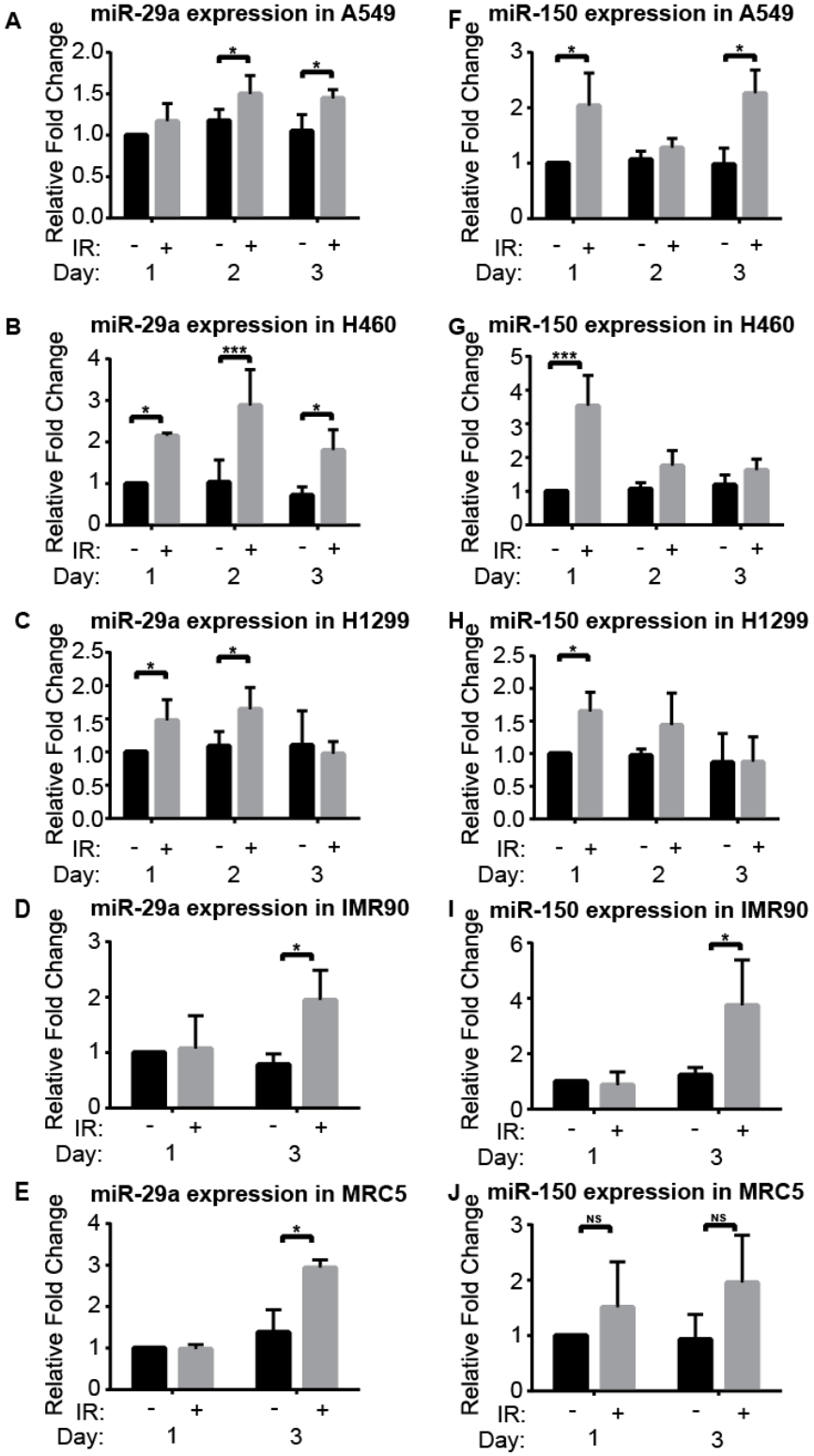

Figure 5. Exosome isolation: Western blot of conditioned media from MRC5 cells after 26 hours of cell culture, with and without radiation. Dark bands show Tsg101 (56 kDa) protein levels in the isolated exosome pellet (left) compared to the supernatant (right).

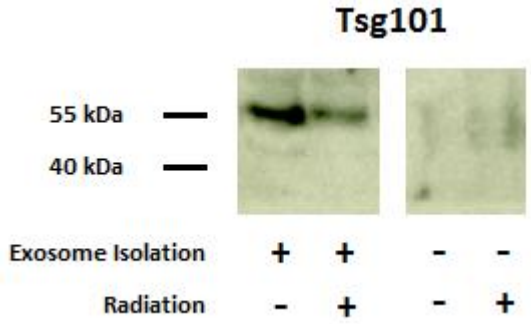

Figure 6. Exosomal expression of miR-29a and miR-150 decreased in both NSCLC and stromal cell lines after 1 or 3 days of 2 Gy fractions. Error bars represent standard deviation (* $p<0.05$, *** $p<0.001$).

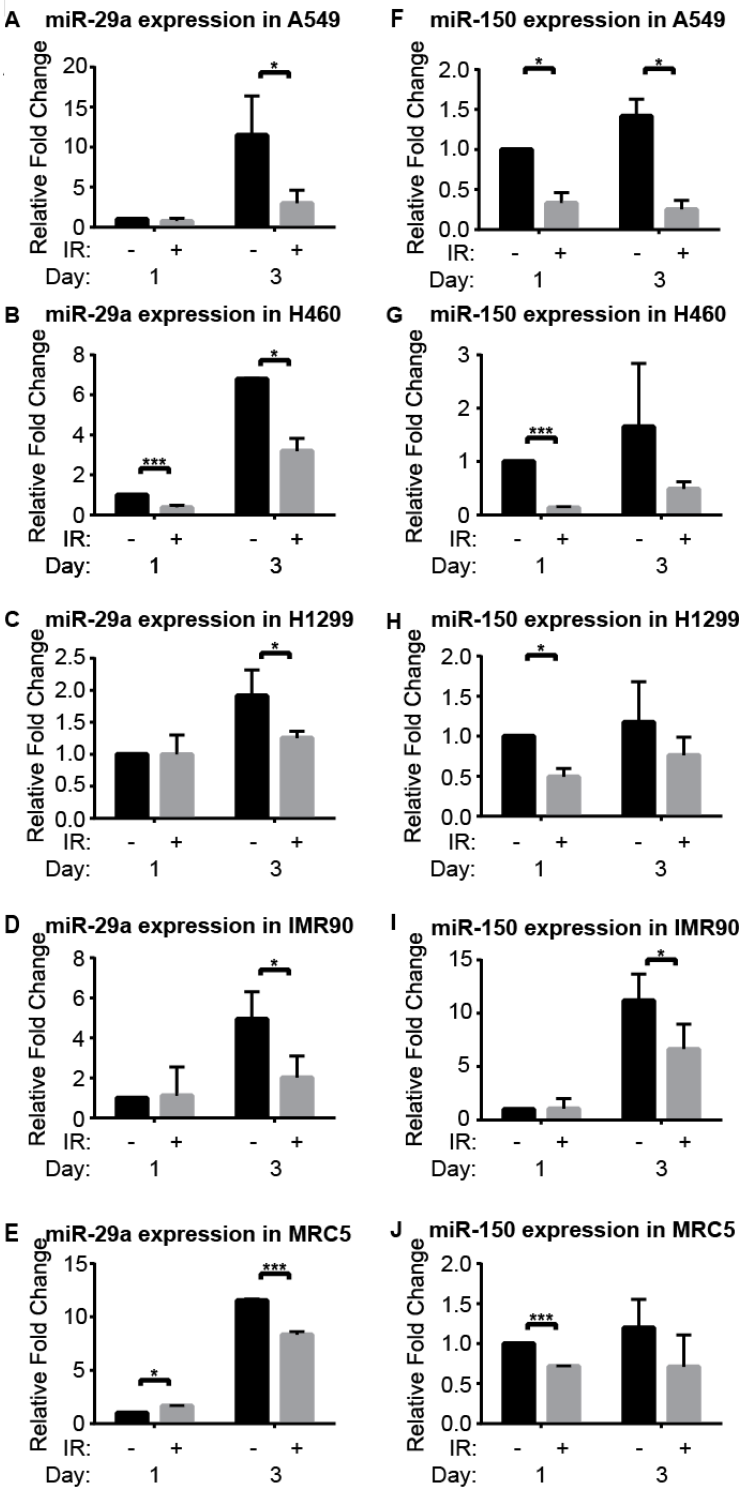

Figure 7. Viability vs. IR status. (A) Irradiation at 2 Gy fractional doses does not significantly decrease cell viability. There was no statistical difference in cell viability in any comparisons between groups. (B) Radiation decreases cell proliferation compared to control after a single fraction of 2, 3 or 4 Gy.

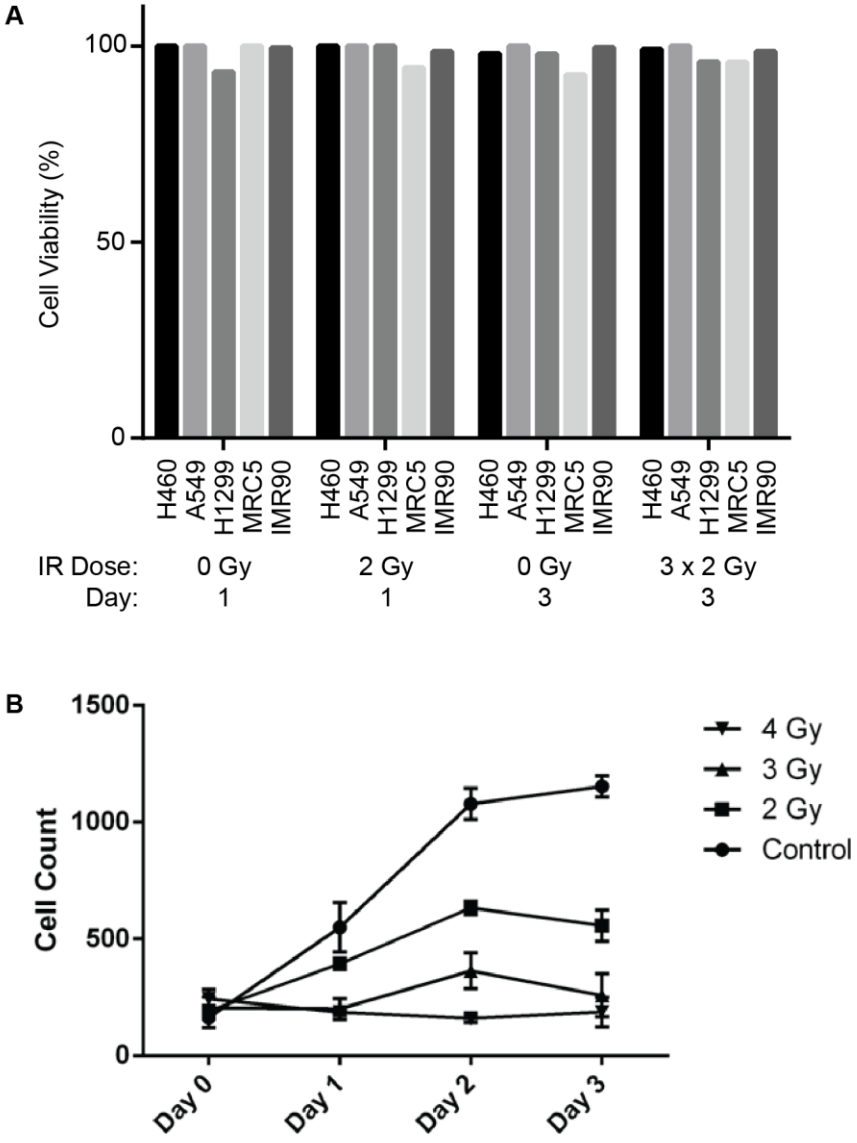

Figure 8. Enrichment plot for gene set enrichment analysis of differences in gene expression in (A) H460 (FDR = 0.158) cells and (B) H1299 cells (FDR = 0.856). In both cases, only genes predicted to be targets of miR-29a were enriched. For each plot, the top portion shows the running enrichment score (ES) for the gene set over every gene in the entire dataset. The middle portion shows where members of the gene set appear in a ranked list of all genes (hits). The bottom portion of the plot shows the ranking metric (postive values indicates correlation with the unirradiated phenotype while negative values indicates correlation with the irradiated phenotype).

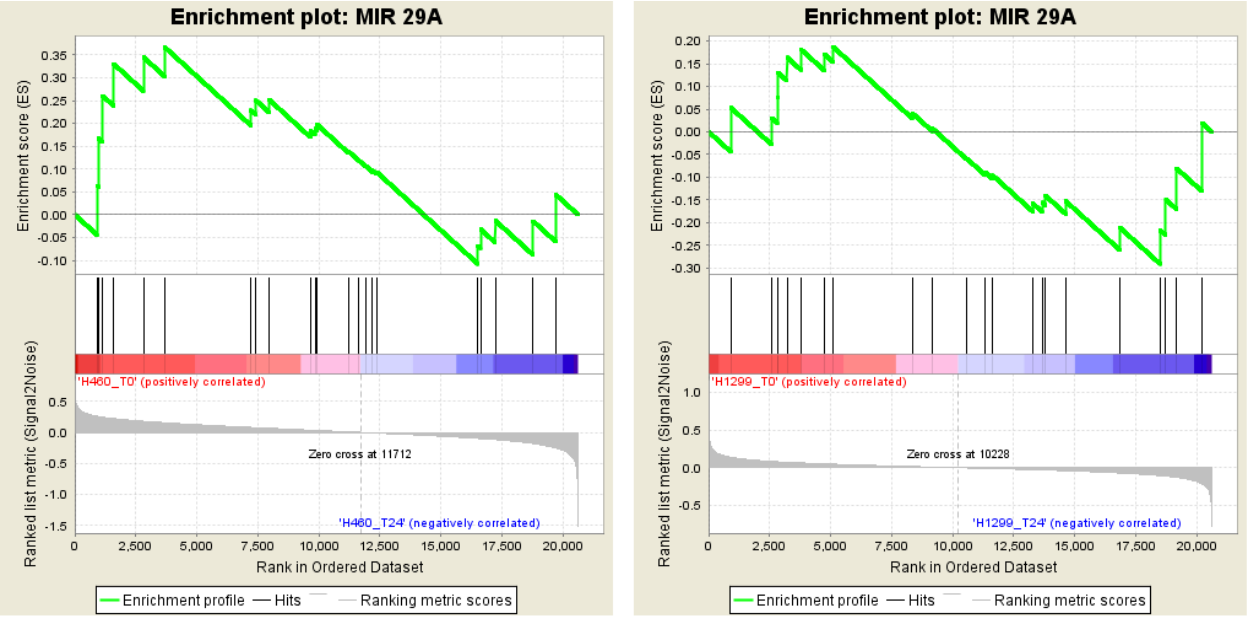

(A) H460 **(B) H1299**

Figure 9. miRNA expression in NSCLC and lung samples. miRNA SEQ data from TCGA database of 504 patient samples. miRNA expression profiles of 456 lung tumor specimens and 48 normal lung specimens were examined. On average, miR-29a and miR-150 are highly expressed (compared to the global average expression) in both normal and tumor tissues. Other miRNAs including miR-342 were not highly expressed. Error bars indicate 95% confidence interval of all data.

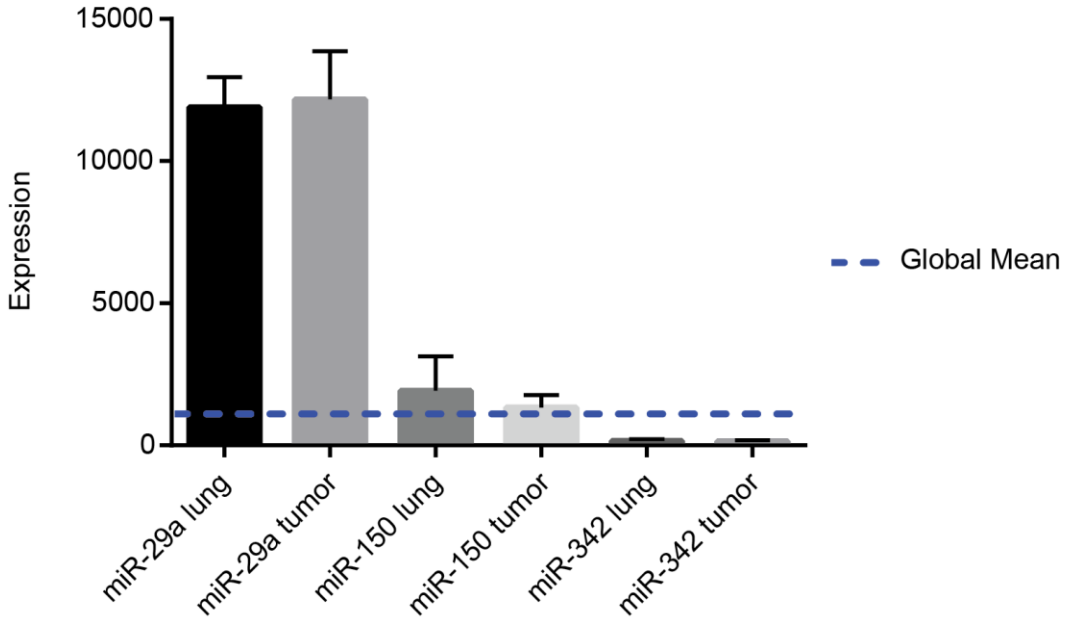

Figure 10. Clinical schematic of circulating miRNAs as biomarkers of thoracic radiation therapy. In this scenario, overexpression of a miRNA biomarker predicts toxicity and allows for reduction of total dose while underexpression predicts radioresistance and allows for dose-escalation.